

Components of polarization-transfer to a bound proton in a deuteron measured by quasi-elastic electron scattering

D. Izraeli^{a,*}, I. Yaron^a, B.S. Schlimme^b, P. Achenbach^b, H. Arenhövel^b, A. Ashkenazi^a, J. Beričić^c, R. Böhm^b, D. Bosnar^d, E.O. Cohen^a, M.O. Distler^b, A. Esser^b, I. Friščić^{d,1}, R. Gilman^e, I. Korover^{a,f}, J. Lichtenstadt^a, I. Mardor^{a,g}, H. Merkel^b, D.G. Middleton^b, M. Mihovilović^{c,b}, U. Müller^b, M. Oliveboim^a, E. Piasezky^a, J. Pochodzalla^b, G. Ron^h, M. Schoth^b, F. Schulz^b, C. Sfienti^b, S. Širca^{i,c}, S. Štajner^c, S. Strauch^j, M. Thiel^b, A. Tyukin^b, A. Weber^b, for the A1 Collaboration

^a*School of Physics and Astronomy, Tel Aviv University, Tel Aviv 69978, Israel.*

^b*Institut für Kernphysik, Johannes Gutenberg-Universität, 55099 Mainz, Germany.*

^c*Jožef Stefan Institute, 1000 Ljubljana, Slovenia.*

^d*Department of Physics, University of Zagreb, HR-10002 Zagreb, Croatia.*

^e*Rutgers, The State University of New Jersey, Piscataway, NJ 08855, USA.*

^f*Department of Physics, NRCN, P.O. Box 9001, Beer-Sheva 84190, Israel.*

^g*Soreq NRC, Yavne 81800, Israel.*

^h*Racah Institute of Physics, Hebrew University of Jerusalem, Jerusalem 91904, Israel.*

ⁱ*Faculty of Mathematics and Physics, University of Ljubljana, 1000 Ljubljana, Slovenia.*

^j*University of South Carolina, Columbia, South Carolina 29208, USA.*

Abstract

We report the first measurements of the transverse (P_x and P_y) and longitudinal (P_z) components of the polarization transfer to a bound proton in the deuteron via the ${}^2\text{H}(\vec{e}, e'\vec{p})$ reaction, over a wide range of missing momentum. A precise determination of the electron beam polarization reduces the systematic uncertainties on the individual components to a level that enables a detailed comparison to a state-of-the-art calculation of the deuteron using free-proton electromagnetic form factors. We observe very good agreement between the measured and the calculated P_x/P_z ratios, but deviations of the individual components. Our results cannot be explained by medium modified electromagnetic form factors. They point to an incomplete description of the nuclear reaction mechanism in the calculation.

Measurements of the polarization transfer $\vec{P} = (P_x, P_y, P_z)$ from a polarized electron to a bound nucleon by the $A(\vec{e}, e'\vec{p})$ reaction and their comparison to those of a free proton were suggested as a powerful tool to observe modifications in the bound proton structure [1]. These require detailed calculations incorporating nuclear effects. However, it still might be conceptually difficult to separate such effects from internal nucleon structure changes.

The deuteron (${}^2\text{H}$) is the simplest nuclear system, with two loosely bound nucleons. Even though it is often used as a ‘free neutron’ target, measurements on the bound proton in ${}^2\text{H}$ in quasi-elastic kinematics are known to have marked differences in comparison to those on a free proton [2]. Such differences can be ascribed to final state interactions (FSI) and other nuclear effects in the deuteron like meson exchange currents (MEC) and isobar configurations (IC), as well as to nuclear medium modifications of the bound proton electromagnetic form factors (FFs). Since most of the properties of the deuteron are described very well by calculations, it serves also as a benchmark for nuclear theory. As such it is important to establish that present state-of-the-art calculations indeed provide a correct description of

the deuteron. Thus, new high precision polarization transfer data can add important information to further test and improve the calculations, since polarization observables generally provide more sensitive tests.

Measurements of the ratio of the polarization transfer components P_x to P_z (P_x/P_z) to a bound proton in ${}^2\text{H}(\vec{e}, e'\vec{p})$ over a wide region of the proton missing momentum were reported in [3]. Measuring the ratio, instead of the individual components, eliminates many systematic experimental uncertainties, particularly those due to electron beam polarization, and is sensitive to the FF ratio. The theoretical calculation [4] that uses free proton FFs reproduced very well the observed deviations from the free proton ratio, suggesting that they stem mainly from FSI. However, while the ratio of the polarization transfer components is sensitive (almost linearly) to the electromagnetic FFs ratio G_E/G_M , some nuclear effects may cancel out in the ratio. The measured individual polarization transfer components provide a more stringent test of the calculation.

Moreover, it was shown that the deviations of P_x/P_z measured on a bound proton in ${}^2\text{H}$ from that on a free proton, were in very good agreement with similar measurements on heavier nuclei, when using the proton virtuality as a universal parameter for these comparisons [5]. Such comparisons are improved by relating the data of each nucleus to a realistic model of the deuteron data, a process that requires

*Corresponding author

Email address: davidizraeli@post.tau.ac.il (D. Izraeli)

¹Present address: MIT-LNS, Cambridge, MA 02139, USA.

the knowledge of the individual polarization transfer components [6]. We introduce such a model below.

In this work we report a new analysis of the ${}^2\text{H}(\vec{e}, e'\vec{p})$ reaction measured at the Mainz Microtron (MAMI) over a wide range of missing momentum of the struck proton. Results of the polarization transfer ratio P_x/P_z deduced from these measurements were reported in [3]. In the new analysis, the beam polarization that was measured periodically during the experiment was determined in a continuous manner. The achieved accuracy was sufficient for extracting the individual polarization transfer components P_x , P_y and P_z , with a precision that can challenge theory.

The kinematics for the quasi-free elastic scattering off a bound nucleon is shown in Fig. 1. The reaction plane is determined by the momentum transfer (\vec{q}) and the outgoing proton momentum (\vec{p}_p), characterized by the spherical angles θ_{pq} and ϕ_{pq} . The incident and scattered electron momenta that define the scattering plane are indicated by \vec{k} and \vec{k}' . The initial and outgoing proton momenta are indicated by \vec{p}_i and \vec{p}_p , respectively. The missing momentum is $\vec{p}_{\text{miss}} = \vec{q} - \vec{p}_p$. The missing momentum (p_{miss}) is taken to be positive (negative) if a component of \vec{p}_{miss} is parallel (anti-parallel) to the momentum-transfer vector. In the impulse approximation with no FSI one has $\vec{p}_{\text{miss}} = -\vec{p}_i$. Following the convention of [3, 5] the polarization components reported here are perpendicular to the scattering plane (\hat{y}) and in the scattering plane along (\hat{z}) and perpendicular (\hat{x}) to \vec{q} .

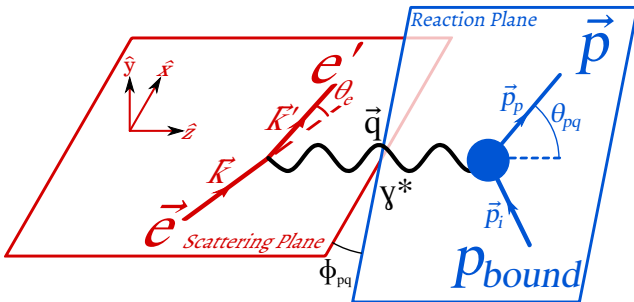


Figure 1: The kinematics for quasi-elastic scattering of a bound proton in a nucleus, defining the scattering and reaction planes.

The experiment was performed on the MAMI A1 beam line using a liquid deuterium target and two of the A1 high-resolution spectrometers [7]. Polarized continuous wave (CW) electron beams of 600 MeV and 630 MeV were used with currents of 10 μA . The target was an oblong cell (50 mm long, 11.5 mm in diameter) filled with liquid deuterium. The spectrometers have momentum acceptances of 20 – 25 % with solid angles of 28 msr and were used to detect the scattered electrons and the knocked out protons in coincidence. The proton spectrometer was equipped with a so called “focal-plane polarimeter” (FPP) placed behind its focal-plane, with a 7 cm thick carbon analyzer [7, 8]. The spin dependent scattering of the polarized proton by the carbon analyzer enabled the determination of the transverse polarization components at the focal plane [8]. The polarization transfer components at the reaction point were ob-

tained by correcting the measured components for the spin precession in the magnetic field of the spectrometer [8].

The measurements covered two Q^2 ranges and two beam energies, in order to span a wide range of p_{miss} . For further details see [9].

The beam polarization at MAMI is obtained by using strained GaAs photocathodes. The beam polarization increases throughout the usage of the single cathode, due to the decrease of its quantum efficiency [10, 11]. The beam polarization was measured daily using a Møller polarimeter located upstream of the target cell. The measurements during the three weeks of the experimental run are shown in Fig. 2, where the slow increase in time is clearly seen. The statistical uncertainty on each measurement is about 1.5%, but there is an overall systematic uncertainty of a few percent, due to the calibration of the detectors in the Møller polarimeter. These measurements were fitted by a linear function ($\chi^2/\text{ndf} = 60.2/61$).

In addition to the Møller measurements, the beam polarization was measured for each beam energy by Mott scattering. The Mott and Møller measurements are consistent (see Fig. 2).

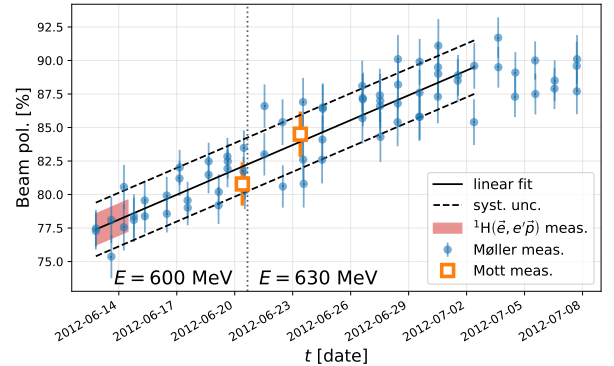


Figure 2: The results of the beam polarization measurements performed with the Møller polarimeter. The linear fit to the data during the data taking period and the uncertainty band are shown as solid and dashed lines. Also shown are the Mott and ${}^1\text{H}(\vec{e}, e'\vec{p})$ measurements. See text for details.

To determine the overall normalization of the beam polarization and the analyzing power, we use measurements of the polarization transfer to a free proton by ${}^1\text{H}(\vec{e}, e'\vec{p})$, which were performed in the beginning of the run (indicated by the red time interval in Fig. 2) at $Q^2 = 0.4 \text{ GeV}^2/c^2$. Assuming the FF ratio G_E/G_M for a free proton from the parameterization of [12] (estimated uncertainty of 0.1%), we deduced the beam polarization from the polarization transfer for these measurements. The resultant overall normalization was 1.00 ± 0.01 . The uncertainty is dominated by the statistical uncertainty of our hydrogen measurements. The band in Fig. 2 shows the overall uncertainty of the beam polarization.

In the analysis of the polarization components, cuts were applied to identify coincident electrons and protons that originate from the deuterium target, and to ensure good reconstruction of tracks in the spectrometers and the FPP. Only events that scatter by more than 10° in the FPP were

selected (to remove Coulomb scattering events in the FPP carbon analyzer). For each event we used the beam polarization obtained from the time-dependence fit.

Time-independent corrections to the polarization transfer measurements (acceptance, detector efficiency, target density, etc.) are largely canceled out by the frequent flips of beam helicity. Contributions to the systematic uncertainty due to the carbon analyzing power and FPP efficiency are well below the statistical uncertainty. The total systematic uncertainties in P_x and P_z are estimated to be about 2% and are due to beam polarization uncertainty (canceled in the P_x/P_z ratio) and the reaction vertex reconstruction (which dominates both the momentum resolutions and the spin-precession evaluation). The systematic uncertainty on P_y is estimated to be comparable to the statistical one.

In our previous analysis [3], where $(P_x/P_z)^{2H}/(P_x/P_z)^{1H}$ was compared to $(P_x/P_z)^A/(P_x/P_z)^{1H}$ in other nuclei, it was shown that the nucleon virtuality, defined as

$$\nu \equiv \left(m_d c - \sqrt{m_n^2 c^2 + p_{\text{miss}}^2} \right)^2 - p_{\text{miss}}^2 - m_p^2 c^2, \quad (1)$$

can serve as a universal parameter for such comparisons. The ratio of the measurements to those of a free proton eliminates some of the variations that are due to kinematics and Q^2 dependence. Using ν as a parameter was shown to give a good universal description of the data, which was further established in new measurements on ^{12}C [5].

We follow this work, and present the ratio of the polarization components P_x and P_z (and their ratio P_x/P_z) to the corresponding values of a free proton as function of ν , in Fig. 3. The proton values were obtained from the global parameterization of Bernauer *et al.* [12]. In the analysis the ratio was taken event by event, and averaged over the virtuality bin. The data in Fig. 3 are shown separately for positive and negative missing momenta to show possible differences predicted by the calculation.

In this analysis, the P_y component of the polarization-transfer, which vanishes for the free proton, was also determined, resulting in very small values. Its consideration is essential for proper determination of P_x and P_z . Since it cannot be compared to the free proton it is not shown in Fig. 3. Also shown in Fig. 3 are the calculated ratios [4]. The calculation uses free proton FFs, and was carried out over the entire data for each event, and averaged over the corresponding bins.

The data indicate that the deviation of $(P_x/P_z)^{2H}/(P_x/P_z)^{1H}$ from unity is mainly due to the P_z component, which according to the calculation, is more sensitive to FSI and relativistic corrections. The calculation is in very good overall agreement with the data. Since medium modifications in the bound proton structure are inferred from deviations of measured data from calculations, a careful comparison between the data and the calculation is necessary.

The comparison was performed by investigating the ratio of the measurements to the calculation event-by-event over the entire data set. These ratios are shown in Fig. 4. The measured P_x/P_z ratio is in very good agreement with the

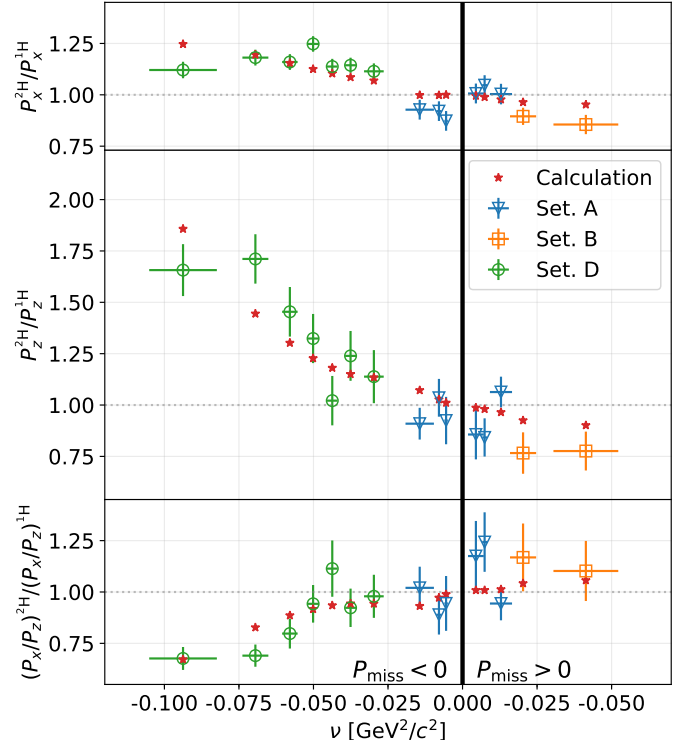


Figure 3: The measured ratios P_x^{2H}/P_x^{1H} , P_z^{2H}/P_z^{1H} and the double-ratio, $(P_x/P_z)^{2H}/(P_x/P_z)^{1H}$, as a function of the proton virtuality, ν . The virtuality dependence is shown separately for positive and negative missing momenta. The symbols for the data of this work correspond to the different kinematical settings, see [9]. Also shown is a calculation for the deuteron [4] (see text for details).

calculation ($p_{\text{value}} = 0.91$). The deviations of about 10% observed in [3] are reduced to less than 1%. This is due to: (a) a comparison of the data with the calculation [4] in the lab frame², (b) improvement of the analysis by using the time-dependent polarization to weigh each event, and (c) a new procedure that compares all three components with the calculation that results in a better overall fit. As can be seen in Fig. 4, we observe differences between the data and the calculation of the P_x and P_z values. Free proton P_x and P_z are functions of the FF ratio G_E/G_M , which become linear for the P_x/P_z ratio. Similarly, for the deuteron, the calculation that uses free nucleon FFs exhibits the same behavior. The good agreement between the measured and the calculated P_x/P_z ratios indicates no need for modifications in G_E/G_M . This does not exclude modifications of the individual FFs which keep the ratio intact. Excluding FF modifications, the deviations of the measured individual components from the calculated ones, suggest that the nuclear effects and/or relativistic corrections included in the calculation should be improved.

Comparisons of polarization transfer data amongst several nuclei are improved by relating the data of each nucleus to a realistic model of the deuteron data, a process that re-

²We note that in [3] the data (in the laboratory frame) were compared to the calculation in the c.m. frame resulting in a 10% discrepancy. A correct comparison will reduce the deviation to about 5%.

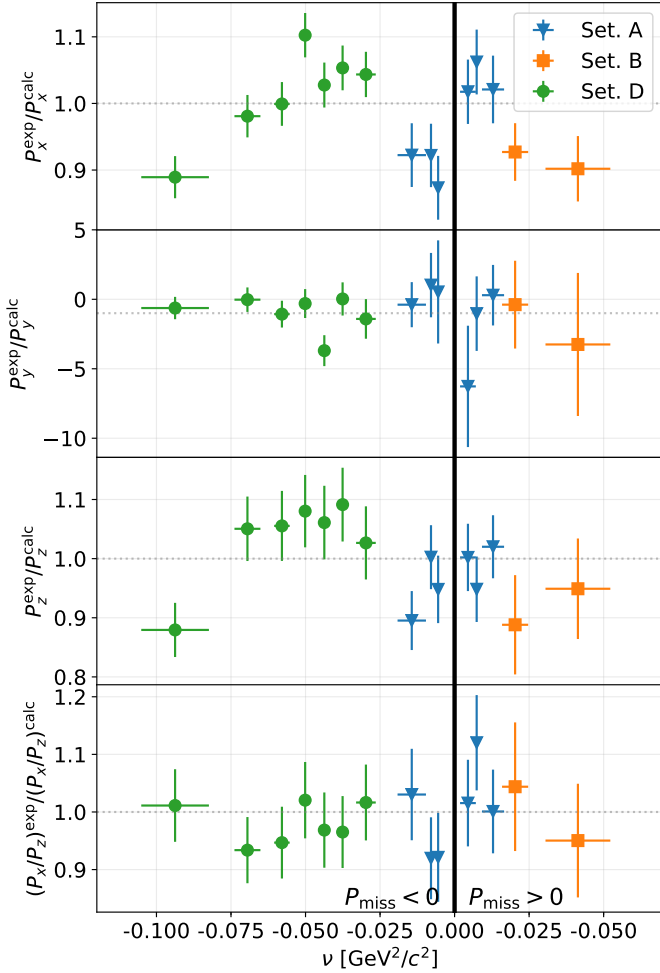


Figure 4: The ratio of the measured to calculated [4] polarization transfer ratios for the components: P_x , P_y , P_z and the ratio P_x/P_z (top to bottom panels, respectively). We use the same symbols as in Fig. 3.

quires the knowledge of the individual polarization transfer components [6]. The accuracy of this process is limited if one averages the results within finite size bins. Using a continuous parameterization of the ^2H data was found to have significant advantages and to be very useful for such a comparison with the ^{12}C data [5]. We introduce in Fig. 5 a parameterization of the data as a function of the nucleon virtuality. The number of fitted parameters was optimized to avoid over-fitting. Shown are the ratios of the individual components to those of the free proton, as well as the double ratio $(P_x/P_z)^{2\text{H}}/(P_x/P_z)^{1\text{H}}$, which were obtained by using multiplication factors to adjust the calculation to the data on an event by event basis. Also shown are the calculations with different ingredients as well as the full calculation [4], from which one can infer that the main deviation from the free proton is due to FSI, as can be seen by comparing the PWBA and DWIA curves. The full parameterization of the data is available in [9].

To summarize, we combined our beam polarization measurements with hydrogen measurements to reduce the uncertainty on the beam polarization. This enables the determination of the individual components P_x , P_y and P_z of

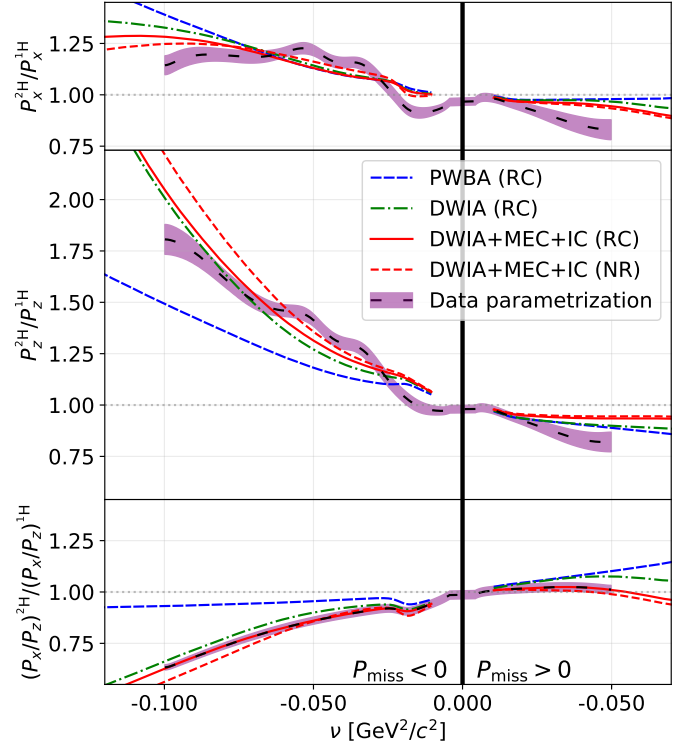


Figure 5: Calculations of [4] with FSI (DWIA) and without (PWBA), with first order relativistic corrections (RC), and without (NR). Also shown is the effect of adding MEC and IC corrections. The data parametrization, obtained by using multiplication factors that adjust the calculation to the measurement, is shown as a dashed line with an uncertainty band of one standard deviation.

the polarization transfer with very good precision. The deviations of the measured P_x and P_z from the corresponding values for a free proton show that the observed deviation of the P_x/P_z ratio is mainly due to P_z , which seems to be more sensitive to FSI and relativistic corrections than P_x .

The comparison of our data to the calculation shows very good agreement for the P_x/P_z ratio, but discrepancies in the individual components. These observations rule out FF changes in the calculation (except for modifications which keep the ratio intact) and suggest the need of improved calculations of FSI and relativistic corrections in the deuteron.

While the data cover a relatively wide range in virtuality (and p_{miss}), further extension of the kinematic range, particularly in the positive p_{miss} region, may further challenge calculations, and are thus important to our understanding of the nuclear mechanisms at work.

We would like to thank the Mainz Microtron operators and technical staff for the excellent operation of the accelerator. This work is supported by the Israel Science Foundation (Grant 390/15) of the Israel Academy of Arts and Sciences, by the Israel Ministry of Science, Technology and Space, by the Deutsche Forschungsgemeinschaft (Collaborative Research Center 1044), by the Slovenian Research Agency (research core funding No. P1-0102), by the U.S. National Science Foundation (PHY-1505615), and by the Croatian Science Foundation Project No. 1680.

References

- [1] C. F. Perdrisat, et al., Nucleon Electromagnetic Form Factors, *Prog. Part. Nucl. Phys.* 59 (2007) 694–764. [doi:10.1016/j.ppnp.2007.05.001](https://doi.org/10.1016/j.ppnp.2007.05.001).
- [2] B. Plaster, et al., Measurements of the neutron electric to magnetic form factor ratio G_E^n/G_M^n via the ${}^2\text{H}(\vec{e}, e'\vec{n}){}^1\text{H}$ reaction to $Q^2 = 1.45(\text{GeV}/c)^2$, *Phys. Rev. C* 73 (2006) 025205. [doi:10.1103/PhysRevC.73.025205](https://doi.org/10.1103/PhysRevC.73.025205).
- [3] I. Yaron, D. Izraeli, et al., Polarization-transfer measurement to a large-virtuality bound proton in the deuteron, *Physics Letters B* 769 (2017) 21 – 24. [doi:10.1016/j.physletb.2017.01.034](https://doi.org/10.1016/j.physletb.2017.01.034).
- [4] H. Arenhövel, W. Leidemann, E. L. Tomusiak, General survey of polarization observables in deuteron electrodisintegration, *Eur. Phys. J. A* 23 (2005) 147–190. [doi:10.1140/epja/i2004-10061-5](https://doi.org/10.1140/epja/i2004-10061-5).
- [5] D. Izraeli, et al., Measurement of polarization-transfer to bound protons in carbon and its virtuality dependence, [arXiv:1711.09680](https://arxiv.org/abs/1711.09680).
- [6] D. Izraeli, et al., Polar polarization, In preparation.
- [7] K. Blomqvist, et al., The three-spectrometer facility at MAMI, *Nucl. Instrum. and Meth. A* 403 (2–3) (1998) 263 – 301. [doi:10.1016/S0168-9002\(97\)01133-9](https://doi.org/10.1016/S0168-9002(97)01133-9).
- [8] T. Pospischil, et al., The focal plane proton-polarimeter for the 3-spectrometer setup at MAMI, *Nucl. Instrum. Methods. Phys. Res., Sect. A* 483 (3) (2002) 713 – 725. [doi:10.1016/S0168-9002\(01\)01955-6](https://doi.org/10.1016/S0168-9002(01)01955-6).
- [9] D. Izraeli, et al., Supplemental material.
- [10] K. Aulenbacher, et al., The MAMI source of polarized electrons, *Nucl. Instrum. Methods. Phys. Res., Sect. A* 391 (3) (1997) 498 – 506. [doi:10.1016/S0168-9002\(97\)00528-7](https://doi.org/10.1016/S0168-9002(97)00528-7).
- [11] R. Alley, et al., The stanford linear accelerator polarized electron source, *Nucl. Instrum. Methods. Phys. Res., Sect. A* 365 (1) (1995) 1 – 27. [doi:10.1016/0168-9002\(95\)00450-5](https://doi.org/10.1016/0168-9002(95)00450-5).
- [12] J. C. Bernauer, et al., Electric and magnetic form factors of the proton, *Phys. Rev. C* 90 (1) (2014) 015206. [doi:10.1103/PhysRevC.90.015206](https://doi.org/10.1103/PhysRevC.90.015206).

Components of polarization-transfer to a bound proton in a deuteron measured by quasi-elastic scattering

Supplementary material

D. Izraeli*, I. Yaron, B.S. Schlimme, *et al.*, for the A1 Collaboration

Abstract

We provide in this supplement the kinematics and details of the experimental set-up as well as the continuous presentation of the polarization-transfer described in the paper.

Table 1: The kinematic settings in the experiment. The angles and momenta are the central values for the two spectrometers' settings: p_p and θ_p (p_e and θ_e) are the knocked out proton (scattered electron) momentum and scattering angles, respectively.

Kinematic	Setting		
	A	B	D
Q^2 [GeV ² /c ²]	0.40	0.4	0.18
E_{beam} [MeV]	600	600	630
p_{miss} [MeV/c]	-80 to 75	75 to 175	-220 to -130
p_e [MeV/c]	385	463	398
θ_e [deg]	82.4	73.8	49.4
p_p [MeV/c]	668	495	665
θ_p [deg]	-34.7	-43.3	-39.1
# of events after cuts	210 k	170 k	790 k

*Corresponding author

Email address: davidizraeli@post.tau.ac.il (D. Izraeli)

Table 2: Data parametrization for $P_y^{2\text{H}}$ and the ratios $P_x^{2\text{H}}/P_x^{1\text{H}}$ and $P_z^{2\text{H}}/P_z^{1\text{H}}$ (defined in the paper) as a function of the knocked out proton virtuality, for $p_{\text{miss}} > 0$. $\Delta P^{2\text{H}}/P^{2\text{H}}$ is the parameterization's relative uncertainty for each of the three components. This parametrization is used in Fig. 5.

ν [GeV ² /c ²]	$P_x^{2\text{H}}/P_x^{1\text{H}}$	$P_y^{2\text{H}}$	$P_z^{2\text{H}}/P_z^{1\text{H}}$	$\Delta P^{2\text{H}}/P^{2\text{H}}$
-0.0500	0.829	0.00049	0.821	0.060
-0.0475	0.831	0.00033	0.819	0.056
-0.0450	0.835	0.00042	0.821	0.053
-0.0425	0.842	0.00054	0.825	0.050
-0.0400	0.851	0.00076	0.832	0.048
-0.0375	0.861	0.00106	0.840	0.045
-0.0350	0.871	0.00094	0.850	0.042
-0.0325	0.882	0.00115	0.862	0.038
-0.0300	0.895	0.00121	0.874	0.035
-0.0275	0.907	0.00137	0.887	0.031
-0.0250	0.919	0.00159	0.900	0.027
-0.0225	0.931	0.00129	0.913	0.024
-0.0200	0.941	0.00133	0.926	0.022
-0.0175	0.952	0.00159	0.938	0.020
-0.0150	0.964	0.00213	0.951	0.019
-0.0125	0.976	0.00233	0.965	0.019
-0.0100	0.985	0.00265	0.978	0.019
-0.0075	0.989	0.00178	0.987	0.019
-0.0050	0.989	0.00062	0.992	0.019
-0.0025	0.983	0.00097	0.992	0.018
0.0000	0.973	0.00087	0.984	0.018

Table 3: Data parametrization (see caption of Tab. 2) as a function of the knocked out proton virtuality, for $p_{\text{miss}} < 0$. This parametrization is used in Fig. 5.

ν [GeV ² /c ²]	$P_x^{2\text{H}}/P_x^{1\text{H}}$	$P_y^{2\text{H}}$	$P_z^{2\text{H}}/P_z^{1\text{H}}$	$\Delta P^{2\text{H}}/P^{2\text{H}}$
-0.1050	1.065	0.00273	1.787	0.046
-0.1025	1.102	0.00408	1.804	0.043
-0.1000	1.133	0.00417	1.809	0.041
-0.0975	1.155	0.00401	1.803	0.039
-0.0950	1.171	0.00355	1.788	0.037
-0.0925	1.184	0.00333	1.770	0.035
-0.0900	1.192	0.00328	1.744	0.032
-0.0875	1.195	0.00391	1.714	0.030
-0.0850	1.196	0.00366	1.683	0.027
-0.0825	1.196	0.00340	1.653	0.026
-0.0800	1.193	0.00322	1.619	0.025
-0.0775	1.190	0.00355	1.588	0.025
-0.0750	1.187	0.00319	1.559	0.025
-0.0725	1.184	0.00358	1.531	0.025
-0.0700	1.183	0.00322	1.508	0.025
-0.0675	1.185	0.00349	1.489	0.024
-0.0650	1.189	0.00298	1.474	0.022
-0.0625	1.196	0.00280	1.465	0.021
-0.0600	1.206	0.00246	1.460	0.019
-0.0575	1.217	0.00282	1.457	0.020
-0.0550	1.226	0.00251	1.452	0.022
-0.0525	1.228	0.00257	1.441	0.023
-0.0500	1.218	0.00210	1.415	0.021
-0.0475	1.196	0.00235	1.378	0.019
-0.0450	1.172	0.00214	1.339	0.022
-0.0425	1.156	0.00168	1.310	0.024
-0.0400	1.155	0.00151	1.299	0.022
-0.0375	1.160	0.00119	1.296	0.020
-0.0350	1.158	0.00058	1.284	0.023
-0.0325	1.141	0.00047	1.258	0.026
-0.0300	1.111	0.00009	1.218	0.027
-0.0275	1.073	0.00026	1.170	0.027
-0.0250	1.033	0.00040	1.121	0.027
-0.0225	0.993	0.00093	1.080	0.028
-0.0200	0.949	0.00385	1.047	0.029
-0.0175	0.920	0.00600	1.017	0.030
-0.0150	0.910	0.00510	0.992	0.028
-0.0125	0.912	0.00398	0.980	0.026
-0.0100	0.920	0.00253	0.974	0.023
-0.0075	0.932	0.00181	0.971	0.020
-0.0050	0.946	0.00059	0.968	0.018
-0.0025	0.960	0.00078	0.974	0.017